



# Memorandum

**Date:** 18 Oct 2002

**From:** T. Prokscha

**To:** LEM group

**Phone:** 42 75

**Room:** WLGA / B15

**cc:**

**E-mail:** thomas.prokscha@psi.ch

---

## TRIMSP reflection coefficients for muons

---

This Memo summarizes the reflection coefficients  $R_N$  for  $\mu^+$  impinging on different elements from low charge number  $Z$  to high  $Z$  as calculated by the program TRIMSP [1]. The data are compared with the predictions of a simple scaling rule provided by Thomas et al. [2] that holds for the backscattering of protons, deuterons, tritium,  $\text{He}^+$  and heavier ions under normal incidence. The backscattering coefficients  $R_N$  – defined as the ratio of the number of projectiles reflected to the number of projectiles incident – can be represented by the expression

$$R_N = \frac{A_1 \cdot \ln(A_2 \epsilon + e)}{1 + A_3 \epsilon^{A_4} + A_5 \epsilon^{A_6}}, \quad (1)$$

where  $e$  is the base of natural logarithm ( $= 2.718$ ), the parameters  $A_1$  through  $A_6$  are found by fitting to the data, and the Thomas-Fermi reduced energy  $\epsilon$  is defined as

$$\epsilon = 32.55 \cdot \frac{\mu}{1 + \mu} \cdot \frac{1}{Z_1 Z_2 \sqrt{Z_1^{2/3} + Z_2^{2/3}}} \cdot E_0, \quad (2)$$

with  $\mu = M_2/M_1$ . Here  $E_0$  is the kinetic energy of the projectile in keV,  $M_1$  and  $M_2$  are the masses of the projectile and the target, respectively, and  $Z_1$  and  $Z_2$  denote the charges of the projectile and target atomic nuclei. According to [1] the expression in Eq. 1 “is consistent with the energy transfer mechanism for an unspecified, multi-term powerlaw potential and preserves the particle (and energy) conservation laws at all energies.”

Figure 1 shows the TRIMSP results for backscattering of  $\mu^+$  where I used normal incidence of muons with energies  $E_0$  between 1 keV and 20 keV, a gaussian energy spread of  $\sigma_E = 500$  eV, Anderson-Ziegler inelastic stopping power, Molière elastic scattering, correction factor for Firsov screening length set to 1, and no recoils (sputtering) generated. The backscattering of  $\mu^+$  increases with decreasing projectile energy, but all the muon data fall below the curve predicted by the scaling formula of Eq. 1: the program yields systematically smaller reflection probabilities for  $\mu^+$ , and the variation of the non-metal targets is much larger than for the metals.

In order to arrive at an equal description of the  $\mu^+$  backscattered data I fitted Eq. 1 to *all*  $\mu^+$  data from TRIMSP to determine the  $A_i$ 's. The result is shown in Fig. 2, and the  $A_i$ 's for  $\mu^+$  and for protons and heavier ions are summarized in Table 1.

## Muon reflection probabilities on different elements, TrimSp

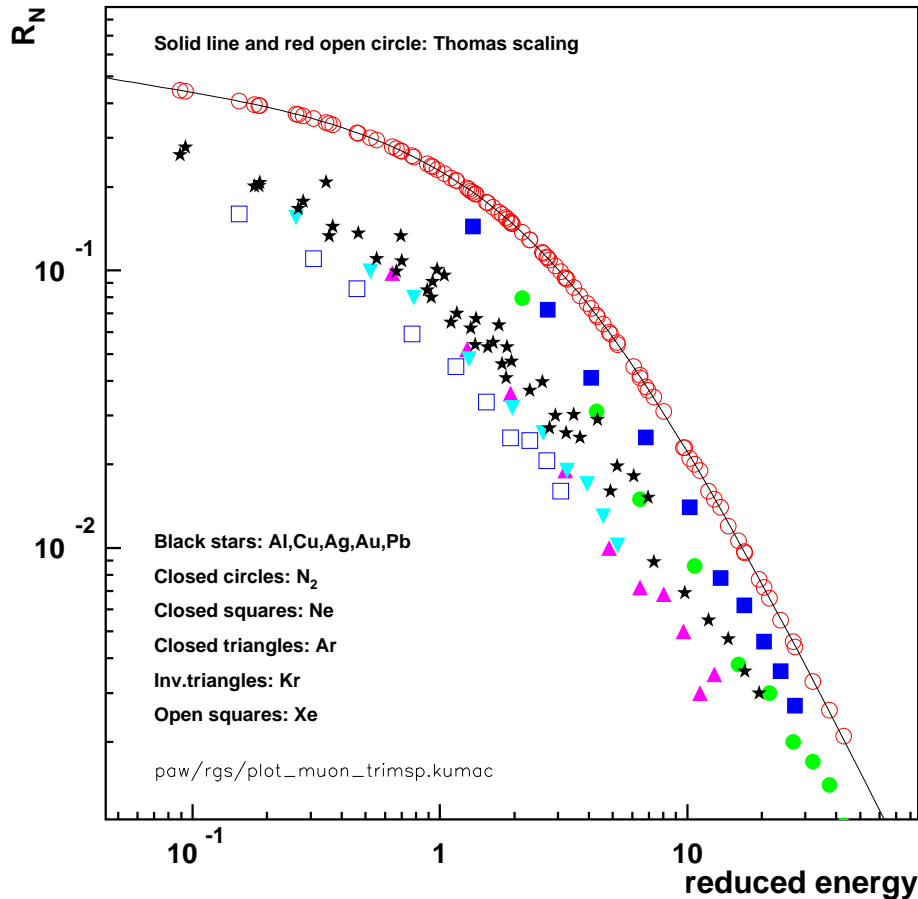


Figure 1: Muon reflection coefficient  $R_N$  as calculated by TRIMSP. The solid line and open circles represent the original Thomas et al. scaling of reflection coefficients for protons and heavier ions [2] which are well reproduced by TRIMSP. The reduced energy  $\epsilon$  is defined in Eq. 2.

### What is the origin of the striking deviation of the TRIMSP $\mu^+$ backscattering data from the Thomas scaling formula ?

This is difficult to say at the moment. Checking the source code of TRIMSP is not an easy task since it is written in “old Fortran” style and not well structured. Therefore it will take some time to understand the details of the source code. But we can get at least one hint: the TRIMSP output gives us the mean energy of the reflected particles. A comparison of the reflected energies for proton, tritium and  $\mu^+$  is shown in Table 2. According to TRIMSP the mean energy of the reflected  $\mu^+$  is significantly smaller than for protons or tritium. This indicates that the energy loss of the backscattered  $\mu^+$  is larger. Due to the larger energy loss the number of backscattered  $\mu^+$  which are stopped before reaching the surface might be higher, thus reducing the reflection coefficient. The question remains open why the energy loss for the  $\mu^+$  should be higher. There is no physical argument for this ?, and it could be caused artificially by the program (the stopping power for  $\mu^+$  in the keV range is

Table 1: Comparison of the original parameters  $A_i$  determined by Thomas et al. [2] with those obtained by fitting Eq. 1 to the  $\mu^+$  backscattering data of TRIMSP.  $\mu$  is the ratio of target mass to projectile mass, see Eq. 2.

| Particle                                   | $A_1$  | $A_2$ | $A_3$ | $A_4$  | $A_5$ | $A_6$ |
|--|--------|-------|-------|--------|-------|-------|
| $\mu^+$ , this Memo, mass range $\mu > 20$ | 0.9504 | 6.344 | 17.41 | 0.7098 | 8.424 | 1.729 |
| Thomas et al., mass range $\mu > 20$       | 0.8250 | 21.41 | 8.606 | 0.6425 | 1.907 | 1.927 |

Table 2: Comparison of the the ratio  $\langle E_R \rangle / E_0$  [(mean energy of reflected particles)/(initial energy)] for  $\mu^+$ , proton (p) and tritium (t) backscattered on aluminum (Al) and gold (Au). The reduced energy  $\epsilon$  as defined by Eq. 2 is quoted in brackets.

| $E_0$     | $\mu^+, \langle E_R \rangle / E_0$ | p, $\langle E_R \rangle / E_0$ | t, $\langle E_R \rangle / E_0$ |
|-----------|------------------------------------|--------------------------------|--------------------------------|
| Al, 1 keV | 0.272 ( $\epsilon = 0.976$ )       | 0.341 ( $\epsilon = 0.940$ )   | 0.344 ( $\epsilon = 0.882$ )   |
| Al, 2 keV | 0.281 ( $\epsilon = 1.953$ )       | 0.329 ( $\epsilon = 1.890$ )   | 0.317 ( $\epsilon = 1.763$ )   |
| Al, 5 keV | 0.253 ( $\epsilon = 4.880$ )       | 0.294 ( $\epsilon = 4.724$ )   | 0.283 ( $\epsilon = 4.407$ )   |
| Au, 1 keV | 0.387 ( $\epsilon = 0.094$ )       | 0.542 ( $\epsilon = 0.093$ )   | 0.590 ( $\epsilon = 0.092$ )   |
| Au, 2 keV | 0.392 ( $\epsilon = 0.187$ )       | 0.516 ( $\epsilon = 0.186$ )   | 0.566 ( $\epsilon = 0.184$ )   |
| Au, 5 keV | 0.355 ( $\epsilon = 0.467$ )       | 0.450 ( $\epsilon = 0.465$ )   | 0.517 ( $\epsilon = 0.461$ )   |

larger than for protons, but this causes a smaller penetration depth, and therefore the way back to the surface for backscattered  $\mu^+$  is shorter, so that for backscattering – to first approximation – the larger stopping power and shorter path way should cancel ?). This could be also a hint for the deviations observed between experimental and TRIMSP data in our implantation studies [3]. In the interpretation of these data we assume that all of the backscattered  $\mu^+$  are completely depolarized due to 100% muonium formation probability in order to explain the decreasing diamagnetic asymmetry with decreasing energy. If the original Thomas scaling is valid for  $\mu^+$  the backscattered  $\mu^+$  fractions would be larger than we thought because TRIMSP yields a much smaller reflection coefficient  $R_N$ . In this case we wouldn't have to require that all of the backscattered  $\mu^+$  are depolarized. But this would mean that experiments on high  $Z$  samples at low implantation energies would be difficult because more than 40% of the  $\mu^+$  would be reflected at 1 keV. However, our Pb measurements in 2001 and 2002 do not show a big decrease in diamagnetic asymmetry with decreasing energy ? Needs some more analysis of the Pb data and other data taken at small implantation energies...

### Reflection coefficients for compounds

For a compound the reflection coefficient can be calculated as well by using Eqs. 1 and 2. The target

## Muon reflection on metals and solid gases, Trimsp

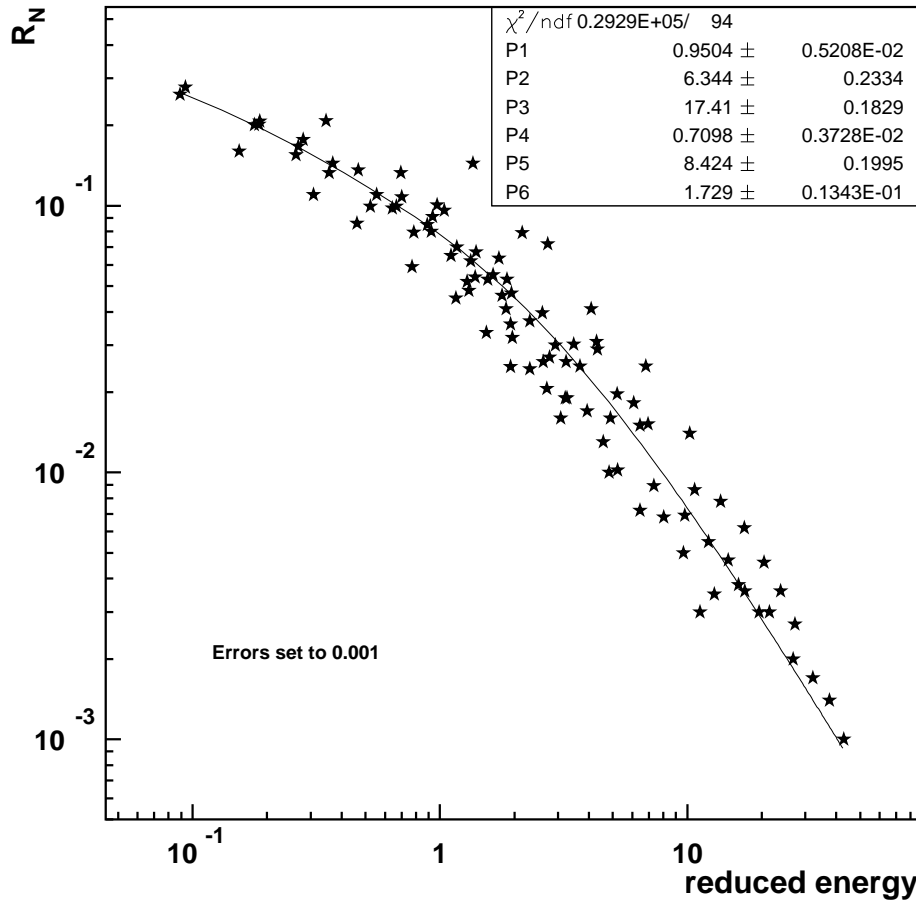


Figure 2: Fit of Eq. 1 to *all*  $\mu^+$  backscattered data of Fig. 1.  $R_N$  is the reflection coefficient and the reduced energy  $\epsilon$  is defined in Eq. 2. The  $P_i$ 's are fit parameter and correspond to the  $A_i$ 's in Eq. 1. They are summarized in Table 1.

atomic charge  $Z$  and mass  $M$  must be replaced by the “effective” charge  $Z'$  and mass  $M'$ :

$$\begin{aligned}
 M' &= \sum_{i=1}^N \frac{n_i}{N} M_i \\
 Z' &= \sum_{i=1}^N \frac{n_i}{N} Z_i,
 \end{aligned} \tag{3}$$

where  $N$  denotes the total number of atoms and  $n_i$  the number of atoms of one species in the compound, and the  $M_i$  and  $Z_i$  are the corresponding masses and nuclear charges. For example, in

SiO<sub>2</sub> the effective mass and charge are given by

$$\begin{aligned}
 M'_{SiO_2} &= \frac{1}{3} \cdot M_{Si} + \frac{2}{3} \cdot M_O = \frac{1}{3} \cdot 28 + \frac{2}{3} \cdot 16 = 20 \\
 Z'_{SiO_2} &= \frac{1}{3} \cdot Z_{Si} + \frac{2}{3} \cdot Z_O = \frac{1}{3} \cdot 14 + \frac{2}{3} \cdot 8 = 10.
 \end{aligned}
 \tag{4}$$

Figure 3 displays the number of  $\mu^+$  implanted in SiO<sub>2</sub> as calculated by TRIMSP and the corresponding curves according to the Thomas scaling. The comparison shows that the use of the effective masses and charges in Eqs. 1 and 2 yields good agreement with the simulated data (as it should be).

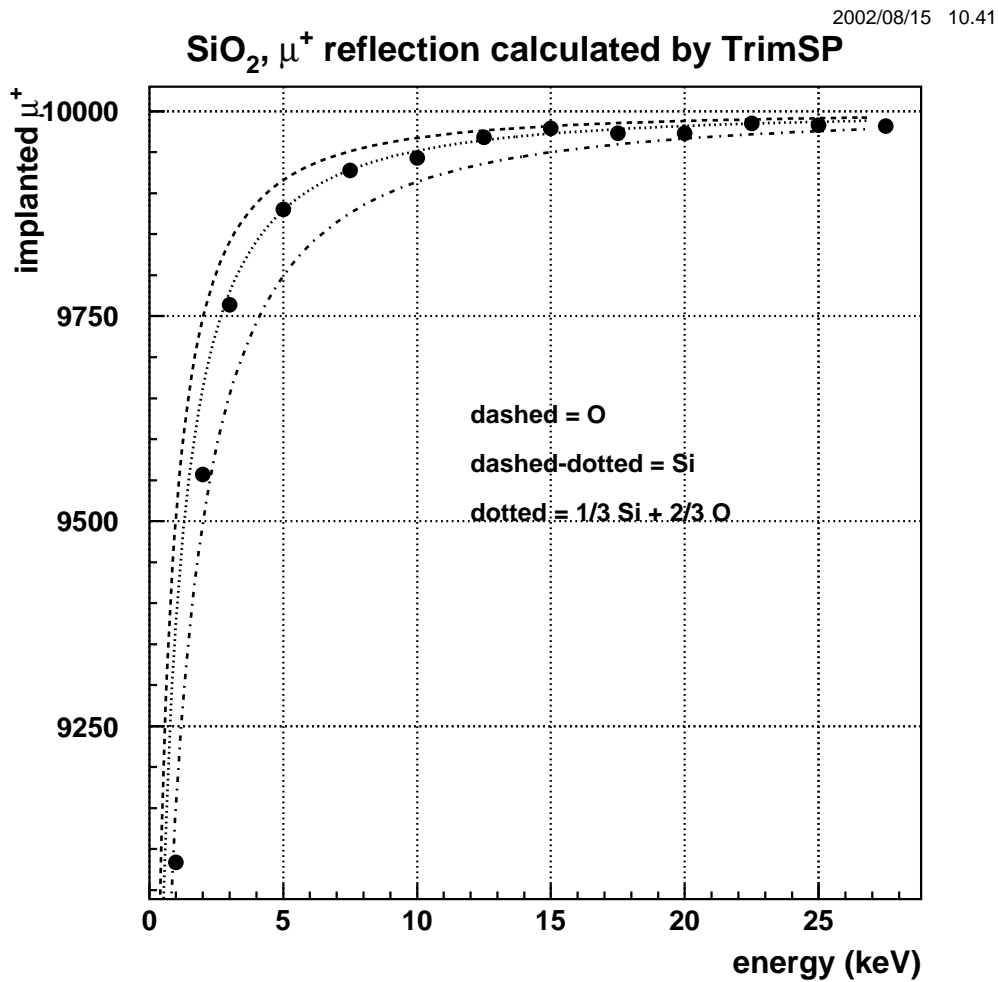


Figure 3: Black circles: number of  $\mu^+$  implanted in SiO<sub>2</sub>, TRIMSP simulation. The curves represent calculations according to Eq. 1 using the modified Thomas parameters for  $\mu^+$  (see Table 1). The dotted curve uses effective masses and charges as quoted in Eq. 3.

## References

- [1] W. Eckstein, *Computer Simulation of Ion-Solid Interactions*, Springer, Berlin, Heidelberg, New York (1991).  
A Linux/Unix version is available under /afs/psi.ch/project/nemu/mc/trimsp. It can be compiled with f77 and needs the CERN `mathlib` at link time for providing the random number generator `ranlux`.
- [2] E.W. Thomas, R.K. Janev and J. Smith, *Scaling of particle reflection coefficients*, NIM B **69**, (1992) 427.
- [3] E. Morenzoni et al., *Implantation studies of keV positive muons in thin metallic layers*, NIM B **192**, (2002) 254.

## Appendix

This section summarizes the TRIMSP simulation data for  $\mu^+$  implanted in several targets taking into account the backscattering at the target. The Figures 4-8 show the comparison of these data with the scaling formula of Eq. 1 where the calculation was done for both, the original Thomas parameters (obtained from proton and heavier ion data) and the modified parameter for  $\mu^+$  as quoted in Table 1.

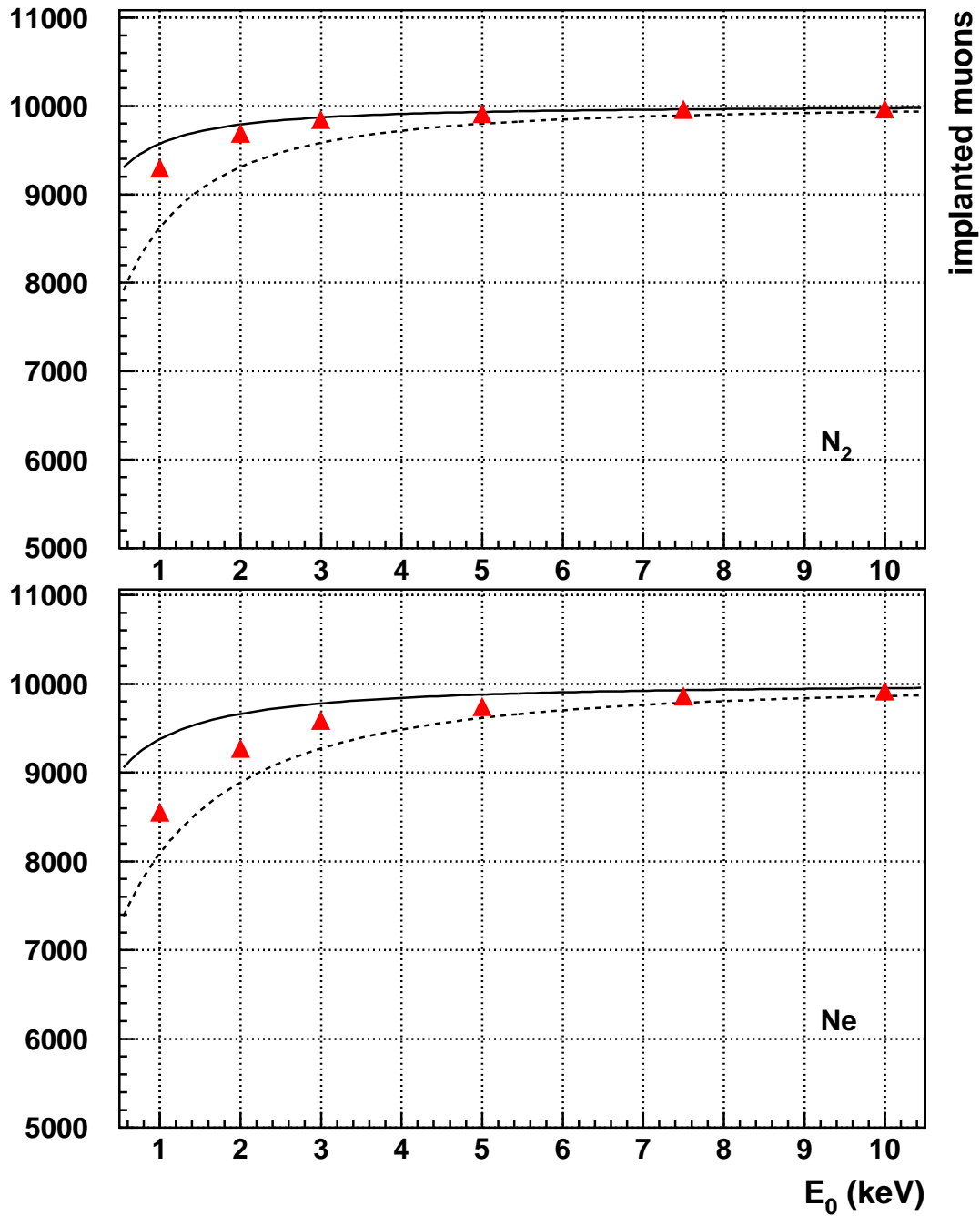


Figure 4: Muons implanted as a function of implantation energy  $E_0$  for nitrogen ( $N_2$ ) and neon (Ne). Triangles: TRIMSP simulation; dashed line: calculation using the original Thomas parameters; solid line: modified Thomas parameters, see Table 1.

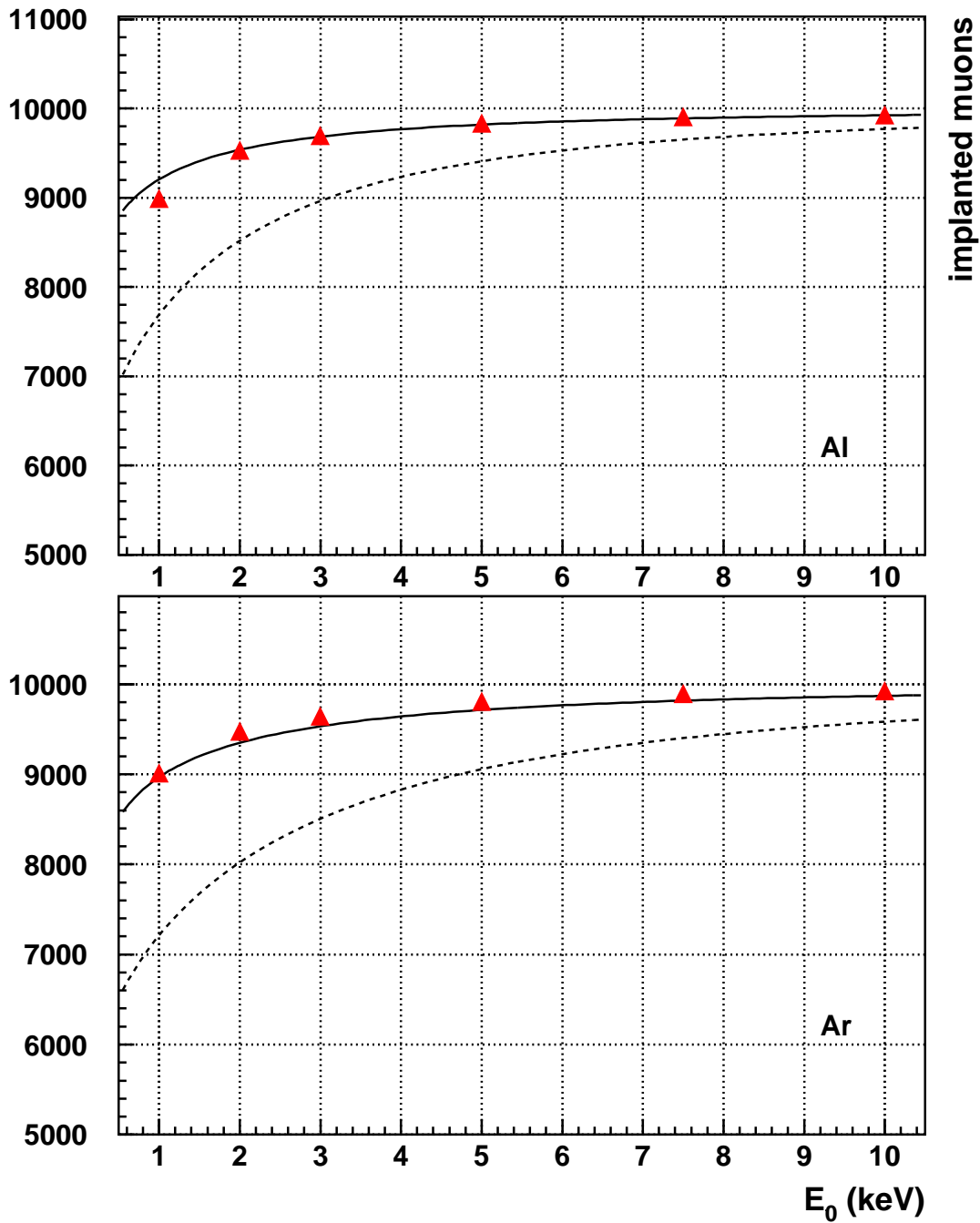


Figure 5: Muons implanted as a function of implantation energy  $E_0$  for aluminum (Al) and argon (Ar). Triangles: TRIMSP simulation; dashed line: calculation using the original Thomas parameters; solid line: modified Thomas parameters, see Table 1.



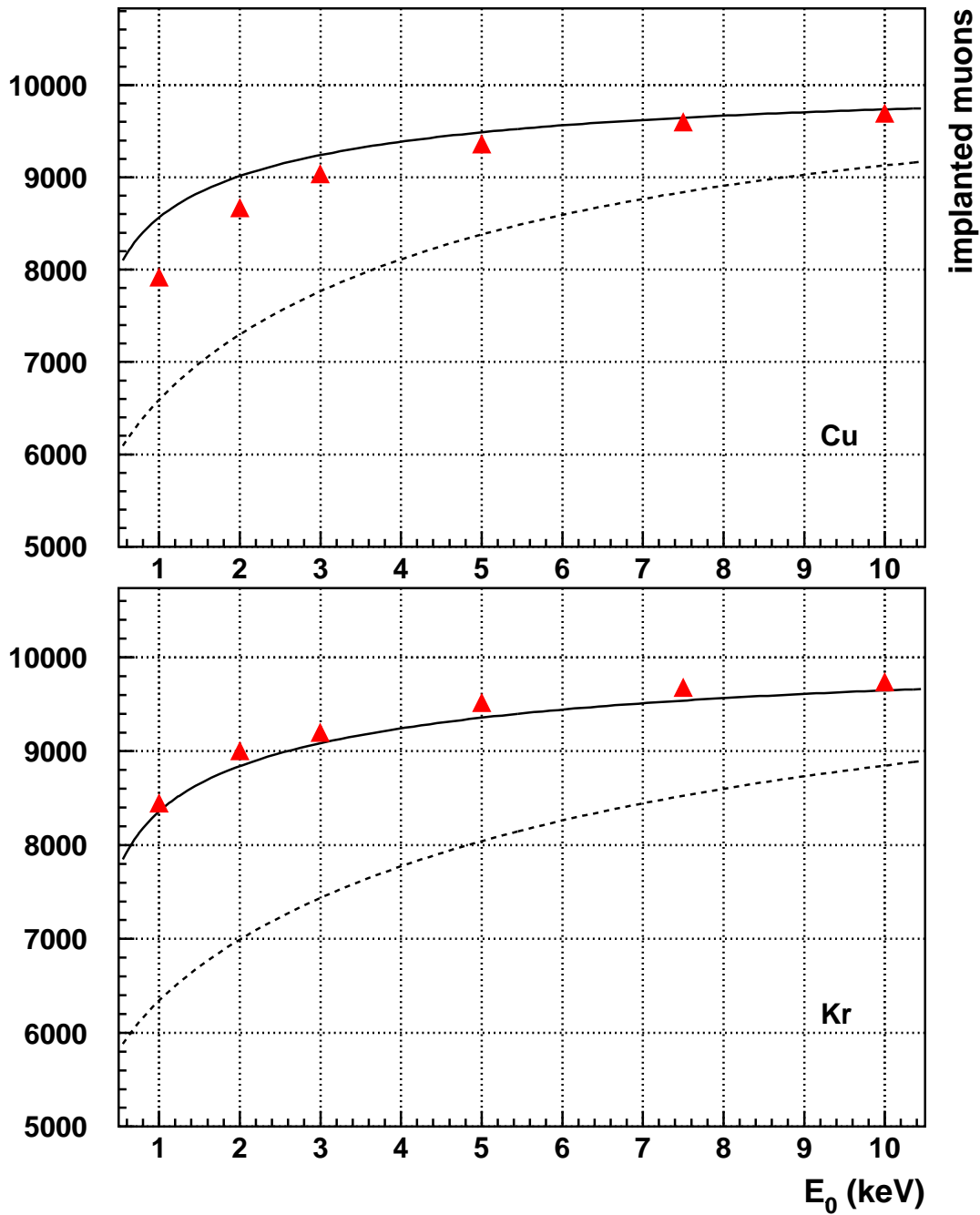


Figure 6: Muons implanted as a function of implantation energy  $E_0$  for copper (Cu) and krypton (Kr). Triangles: TRIMSP simulation; dashed line: calculation using the original Thomas parameters; solid line: modified Thomas parameters, see Table 1.

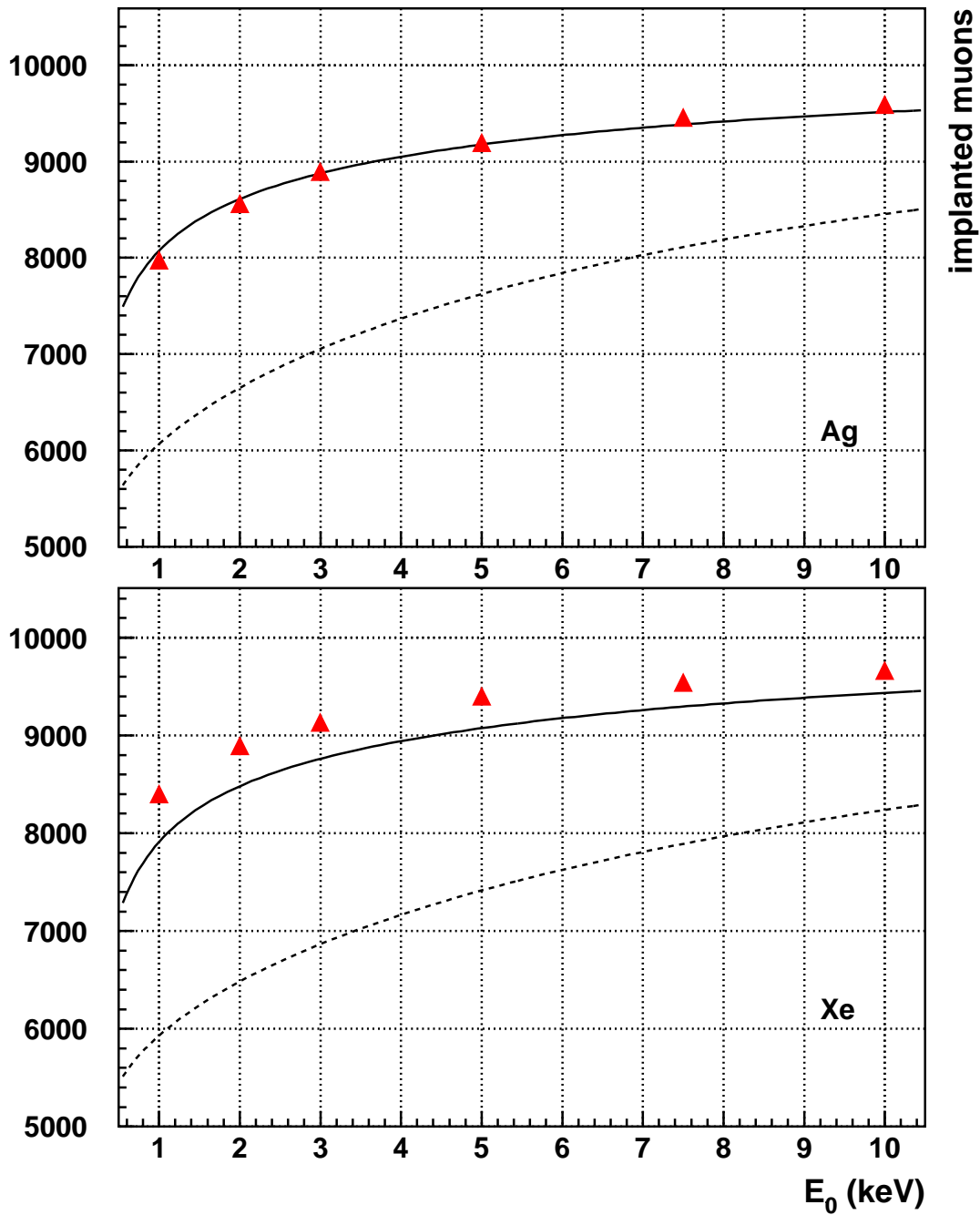


Figure 7: Muons implanted as a function of implantation energy  $E_0$  for silver (Ag) and xenon (Xe). Triangles: TRIMSP simulation; dashed line: calculation using the original Thomas parameters; solid line: modified Thomas parameters, see Table 1.

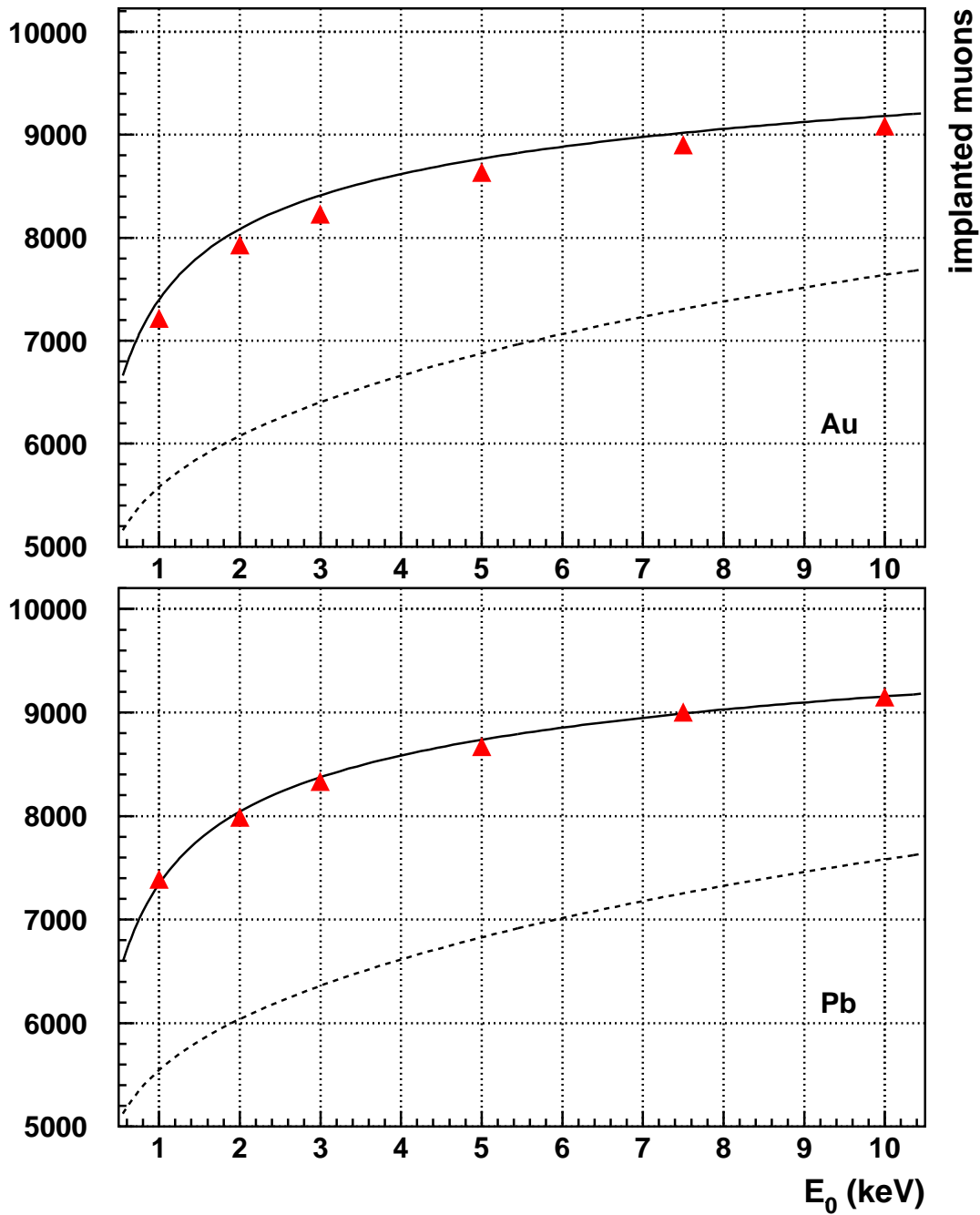


Figure 8: Muons implanted as a function of implantation energy  $E_0$  for gold (Au) and lead (Pb). Triangles: TRIMSP simulation; dashed line: calculation using the original Thomas parameters; solid line: modified Thomas parameters, see Table 1.